Electromagnetic Properties of Periodic Cavities Coupled to a Radiating Antenna

Satoru Kobayashi, M. Botton, Yuval Carmel, *Senior Member, IEEE*, Thomas M. Antonsen, Jr., *Member, IEEE*, John Rodgers, Anatoly G. Shkvarunets, Alexander N. Vlasov, *Member, IEEE*, L. Duan, and Victor L. Granatstein, *Fellow, IEEE*

***Abstract*—The electromagnetic properties of spatially periodic cavities determines both the linear and nonlinear interaction between the waves and the electron beam in high-power backward-wave oscillators. A corrugated cavity is usually left open at one end for extraction of the useful microwave energy; however, reflections at the open end are large so that a cavity is still formed. In contrast to a previously studied N period closed cavity where the number of axial modes with frequencies falling in the lowest pass band of the structure is equal to $N+1$, an open cavity was found to support only N axial modes. In this paper the resonance frequencies, quality factors and the field patterns of the axial modes in an open cavity were all investigated experimentally and the results are in very good agreement with those obtained using a new, time-dependent, quasi-three-dimensional code. It was also demonstrated that a short interface section between the periodic cavity and the radiating antenna can drastically reduce the quality factors to the diffraction limit over a very wide frequency band. This is expected to substantially increase the starting current and allow operation at high-beam current without degradation of spectral purity.**

***Index Terms*— Backward-wave oscillators, high-power microwave, open cavities, periodic cavities, wide-band matching.**

I. Introduction

PERIODIC structures are widely used in microwave radiation sources and charged particle accelerators. Supporting the propagation of slow electromagnetic waves (phase velocity lower than the speed of light), these structures are designed to match the phase velocity of the waves to the velocity of the copropagating electrons, in order to facilitate an effective beam-wave interaction. For generation of microwave radiation, the phase velocity of the wave must be slightly lower than the beam velocity, whereas for particle acceleration, the wave propagates slightly faster than the beam, but its phase velocity is still lower than the speed of light in vacuum. Relativistic backward-wave oscillators (BWO's) are based on such interaction between an electron beam and slow electromagnetic waves [1]–[3]. A linear relativistic electron beam is in synchronism with a slow electromagnetic wave for which the group velocity is in the opposite direction, hence an internal feedback mechanism is formed and self-oscillations are possible. The slow wave structure often consists of a finite-length cylindrically symmetric corrugated wall waveguide operating in the TM_{01} mode. A detailed knowledge of the cold-mode characteristics (i.e., with no electron beam) of the periodic cavity is essential for the design of an efficient BWO. This includes the resonant frequencies associated with the different axial modes, their quality factors, the dispersion properties (namely phase and group velocities) as well as detailed specification of the field patterns.

Closed periodic cavities are formed when a finite section with N periods of the corrugated waveguide is shorted at both ends. When the reflecting planes are placed at the wide section of the periodic waveguide, there are $N+1$ distinct resonances (axial modes) in the first half of the Brillouin zone [4], [5], equally spaced between $k_z d = 0$ and $k_z d = \pi$ (here k_z is the longitudinal wave-number and d is the period of the structure). For example, a closed periodic cavity with six periods ($N = 6$) is characterized by seven axial modes in the region $0 \leq k_z d \leq \pi$, and each one is distinguished by a different axial wave-number, namely $k_z d = n\pi/6$ ($n = 0, 1, \cdots, 6$ is the index of the axial mode). The pattern of the electromagnetic field is essentially given by the form of the fields that propagate in the infinitely long periodic structure, multiplied by an envelope function which will satisfy the boundary condition at the two ends. Thus for example, the transverse electric field in a closed periodic cavity of length $L = 6d$, has an envelope function of the form $\sin[(z/d)(n\pi/6)]$, where we have [5] and [6].

However, a practical corrugated cavity used in a relativistic BWO is intentionally left open at one end, to allow for extraction of the useful microwave energy into a radiating antenna or a load. In many cases, the beam input end is terminated by a waveguide section in which the dominant mode is below cutoff, and not by a conducting plate as in the closed cavity. We shall refer to this cavity as an "open periodic cavity." In the absence of the strict boundary conditions defined by a metallic plate, substantial changes in the electromagnetic properties of the cavities are expected. The frequencies, quality factors, and field pattern of the axial modes in open cavities are all expected to change. Moreover, each axial mode is expected to be affected in a different way. These changes may influence the properties of the interaction between the waves and the electron beam, both in the linear regime (e.g., frequency of operation, coupling impedance, start-oscillation current), and the nonlinear regime (e.g., efficiency, spectral purity of the radiation field) [7]. In this context, theoretical and experimental studies of the properties of open periodic cavities are essential.

Manuscript received September 12, 1997; revised January 14, 1998. This work was supported by the Air Force Office of Scientific Research (MURI-94: Research on Compact, High Energy Microwave Sources).

The authors are with the Institute for Plasma Research, University of Maryland, College Park, MD 20742 USA.

Publisher Item Identifier S 0093-3813(98)04277-5.

Previous studies of an open periodic cavity [8]–[10], were based on the assumption that the field in the cavity can be described by an envelope function multiplying the field of an infinitely long periodic structure. The boundary conditions at the open ends were formulated by means of an effective reflection coefficient that related the forward and backward propagating waves. In [8] and [9] the reflection coefficients were assumed to be frequency-independent. This is an acceptable assumption as long as the operation-frequency is not close to the π-frequency. The start-oscillation currents were calculated for several values of reflection coefficients. The near-cut-off operation case was addressed in [10]. The reflection coefficient was evaluated using a numerical model for a semiinfinite periodic structure [11], and the start-oscillation current were determined. Nevertheless, when a matching section (the open end of the cavity) is tapered these analysis techniques are insufficient, and a more detailed understanding of the electromagnetic modes is required.

A second motivation for the present work is the interest that has developed around wide band, tunable high power microwave (HPM) sources employing either evacuated [12], [13] or plasma loaded slow wave structures [14]–[18]. In these cases, there is often a need to reduce the quality factor (Q) of an "open" corrugated cavity over as wide-frequency band, by reducing the end reflection coefficient (R) in order to achieve optimal coupling to an antenna. In the present work, we demonstrate that a short wide-band high-power corrugated matching section, can be used as an interface between the cavity and the antenna.

Perturbation techniques are available for measuring the spatial distribution of fields in resonant cavities [19]–[21]. These techniques have been primarily applied to closed high Q (often over 4000) cavities. In contrast, spatially periodic open cavities intended for operation with intense relativistic beams have not been studied in detail. The electromagnetic properties of these open corrugated cavities is the main focus of the present work. A single port reflection technique (S_{11}) to measure the discrete resonance frequencies associated with the various axial modes of the open cavity was used, and a perturbation technique to characterize the field profile of each of the individual axial modes.

This paper is structured as follows. The experimental apparatus for performing those measurements is described in the next section. The measured properties were compared with numerical calculations (using MAGIC [22] and the newly developed MAGY [23] codes). Both the experimental and simulations results will be presented in Section III. In Section IV we present the results of our studies aimed at substantially reducing the Q of corrugated open cavities by employing a short wide bandwidth matching section between the cavity and the microwave radiating antenna. Finally, we present a short summary in Section V.

II. Experimental Setup and Theoretical Background

There are three levels at which the experimental results can be compared with the numerical simulation. The first and simplest level is to compare the measured and calculated resonant frequencies of each of the axial modes in an open cavity which are associated with the TM_{01} transverse mode. The second is to compare the measured and calculated quality factors of the same modes. The third, and most challenging, is to compare the measured and calculated field distribution (or the related spatial distribution of frequency shifts) of these axial modes. In Section III we shall present the comparison on all the three levels.

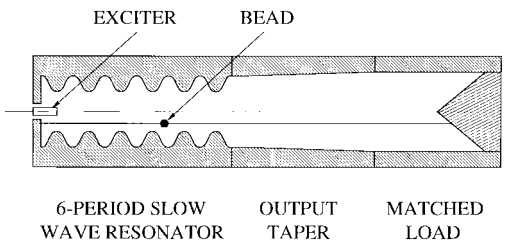

Fig. 1. A schematic diagram of the open periodic cavity and the experimental setup used for the frequency and field profile measurements (see text for details). $R_{\rm wall} = R_0 + h\cos(2\pi z/d)$ where $R_0 = 1.494$ cm, $h = 0.401$ cm, and $d = 1.67$ cm.

The open cavity consisted of six period corrugated wall copper waveguide with a wall radius described by $R_{\rm wall} = R_0 + h\cos(2\pi z/d)$, where $R_0 = 1.49$ cm, $h = 0.401$ cm, and $d = 1.67$ cm. The structure was made of three copper sections compressed together to ensure good electrical contact. The microwave radiation was extracted into a matched load through an over-moded smooth waveguide. This arrangement, shown in Fig. 1, mimics the coupling of the cavity to a radiating antenna. Under these conditions, the quality factor of the cavity is dominated by the radiation extraction and not by the ohmic wall losses.

The modes in the open cavity were excited using a small, on the axis, Hertzian exciter (Fig. 1). A network analyzer was used to measure the microwave reflection from the open cavity over the desired frequency range (7.2–9.0 GHz) using an S_{11} single port measurement. The resonances appear as narrow spikes at frequencies where the magnitude of the reflection was reduced.

The quality factor measured experimentally (Q_L) includes the loading effect of the exciter. The exciter loading therefore must be evaluated and properly isolated so that the measurement will reflect the actual Q value of the open cavity itself. We measured the voltage standing wave ratio (VSWR) of the open cavity across the desired resonance using a HP8510C vector network analyzer. From this data we found the minimum VSWR (at resonance) and maximum VSWR (between resonances). From these two values we used a technique [24], [25] to find the VSWR level at which to read the upper and lower frequencies, f_1 and f_2, of each resonance. From these frequencies, and the resonant frequency f_r we can calculate the open cavity Q by removing the coupling effect from the loaded $Q_L = f_r/(f_1 - f_2)$.

To measure the spatial distribution of frequency shifts in an open cavity we used a perturbation technique. A small spherical aluminum bead (0.24 mm diameter) located at a radial position of 0.53 cm (expected electron beam location) was translated parallel to the cavity axis by steps of 0.25

mm and the resulting frequency shifts of each axial mode were measured as a function of its position. Fig. 1 shows a schematic diagram of the apparatus. This method is widely used to measure field profile in closed Q cavities [3] and is used here, for the first time in an open low Q environment [5].

In the past, perturbation techniques were used to analyze field patterns on closed cavities, where the power flow out of the cavity is zero. In this work we tried to apply the same approach to an open cavity in which the energy loss due to radiation coupling is much larger than the ohmic wall losses. For the theoretical justification of perturbation technique in open cavities, we repeat the perturbation analysis [19]–[21], [24], [25], taking into consideration the power flow out of the cavity. We start by assuming that the open cavity is excited at the *resonant* circular frequency ω. The unperturbed fields satisfy (in c.g.s. units)

$$\nabla \times \boldsymbol{E}_0 = ik_0\eta_0\boldsymbol{H}_0 \tag{1a}$$

$$\nabla \times \boldsymbol{H}_0 = -ik_0\frac{1}{\eta_0}\boldsymbol{E}_0 \tag{1b}$$

where $k_0 \equiv \omega/c, \eta_0 = \sqrt{\mu_0/\varepsilon_0}$ is the plane wave impedance and c is the speed of light in vacuum. We assume that the sources are located on the boundary of the cavity (e.g., a small pin exciter, see Fig. 1). The presence of the spherical bead (radius a) introduces a small perturbation to the resonant frequency and the profile of the fields, namely $k = k_0 + \delta k$ and $\boldsymbol{E} = \boldsymbol{E}_0 + \boldsymbol{E}_1, \boldsymbol{H} = \boldsymbol{H}_0 + \boldsymbol{H}_1$. The perturbed fields satisfy

$$\nabla \times \boldsymbol{E}_1 = i(k_0 c\boldsymbol{B}_1 + \delta k\eta_0\boldsymbol{H}_0 + \delta kc\boldsymbol{B}_1) \tag{2a}$$

$$\nabla \times \boldsymbol{H}_1 = -i\left(k_0 c\boldsymbol{D}_1 + \delta k\frac{1}{\eta_0}\boldsymbol{E}_0 + \delta kc\boldsymbol{D}_1\right) \tag{2b}$$

where $\boldsymbol{D}_1 = \varepsilon_0\boldsymbol{E}_1 + \boldsymbol{P}_1, \boldsymbol{B}_1 = \mu_0\boldsymbol{H}_1 + \boldsymbol{M}_1$, and $\boldsymbol{P}_1, \boldsymbol{M}_1$ are the equivalent polarization and magnetization vectors, respectively. We now multiply (2a) by the complex conjugate $\boldsymbol{H}_0^*$ and (2b) by $\boldsymbol{E}_0^*$, add them, and integrate over the volume of the cavity. Grouping terms of k_0 and δk, we get (3), shown at the bottom of the page. The first term of the numerator is of the order of $\approx |\boldsymbol{E}_0|^2 a^3$. The second term in the numerator is an integration over the open end of the cavity, as the tangential components of $\boldsymbol{E}_1$ and $\boldsymbol{E}_0^*$ vanish at the metal walls of the cavity. This term represents the power flux due to the perturbation field. We estimate that this term is smaller than the first term by a factor proportional to the Q of the cavity. Thus for $Q > 100$ it can be neglected. Furthermore, the second term of the denominator is small compared to the first as the contribution to the perturbation field is mostly limited to a volume of the order of which is much smaller than V (the volume of the cavity). Under these assumptions, we find that the frequency shift is given by

$$\frac{\delta f}{f_0} \cong \frac{4\pi a^3\left(\frac{1}{2}|\eta_0\boldsymbol{H}_0(r_b, z_b)|^2 - \left|\frac{1}{\eta_0}\boldsymbol{E}_0(r_b, z_b)\right|^2\right)}{\iiint_V \left(\eta_0|\boldsymbol{H}_0|^2 + \frac{1}{\eta_0}|\boldsymbol{E}_0|^2\right) dv}. \tag{4}$$

This expression, which is identical to the one previously used for closed cavities (see [4]), establishes the theoretical justification for the interpretation of the perturbation method as the axial profile of the field in open cavities. It is important to note that a metallic bead will in general perturb both electric and magnetic field components, and both are included in (4). Therefore, the bead can be placed at an arbitrary position in the cavity, as long as this position is known. The measured data are compared with the calculated values, and the results will be presented in the next section.

As an additional theoretical support, a numerical simulation code (MAGY [23]) was used. This is a time-dependent quasi-three-dimensional code that simulates the interaction between electron beams and electromagnetic waves in circular waveguides with arbitrarily varying radius. In this work we used only the electromagnetic part (no electrons), to compute the fields in the periodic cavity using the same excitation method (a pin exciter on axis). The code calculates the voltage (V) and current (I) amplitudes for the transverse electric (TE) and transverse magnetic (TM) modes using the generalized telegrapher's equations [23]. The fields are computed using these amplitudes for the eigenfunctions of the cavity-modes. We then calculated the frequency shift using (4). In the following section we present the experimental results and the comparison to the numerical simulations.

III. Experimental Results and Numerical Simulations

The resonance frequencies and wavenumbers of the various axial modes associated with the lowest TM_{01} mode as measured for the six-period open cavity are shown in Fig. 2 (solid rectangles ■). For comparison, we also show the equivalent data for the six-period *closed* cavity (open circles ○ see [4] for details). From these figures, it is clearly evident that the closed periodic cavity with $N = 6$ periods supports $N + 1 = 7$ different longitudinal modes, whereas the open periodic cavity supports only $N = 6$ such modes. The seven longitudinal modes of the closed cavity are equally spaced in the half of the first Brillouin zone, the spacing being $\pi/6$. The six longitudinal modes of the open periodic cavity closely conform with the "half-integer" spacing [26], namely the nth longitudinal mode has a normalized wave-number $k_z d/\pi = (n + 1/2)$. The zero $(n = 0)$ and the π $(n = 6)$ modes of the

$$\frac{\delta f}{f_0} \equiv \frac{\delta k}{k_0} = \frac{-ci\iiint_V (\boldsymbol{P}_1 \cdot \boldsymbol{E}_0^* + \boldsymbol{M}_1 \cdot \boldsymbol{H}_0^*)\, dv + \frac{1}{k_0}\iint_A (\boldsymbol{E}_1 \times \boldsymbol{H}_0^* + \boldsymbol{E}_0^* \times \boldsymbol{H}_1) \cdot d\boldsymbol{a}}{i\iiint_V \left(\frac{1}{\eta_0}|\boldsymbol{E}_0|^2 + \eta_0|\boldsymbol{H}_0|^2\right) dv + ci\iiint_V (\boldsymbol{B}_1 \cdot \boldsymbol{H}_0^* + \boldsymbol{D}_1 \cdot \boldsymbol{E}_0^*)\, dv} \tag{3}$$

TABLE I
RESONANCE FREQUENCIES AND QUALITY FACTOR AS MEASURED AT THE EXPERIMENT, AND CALCULATED BY MAGY AND MAGIC CODES

Experiment		MAGY		MAGIC	
f (GHz)	Q	f (GHz)	Q	f (GHz)	Q
7.4295	632	7.4324	665	7.429	>760
7.587	345	7.6081	348	7.590	280
7.875	183	7.8918	182	7.886	163
8.217	195	8.2423	181	8.228	---
8.541	297	8.5945	323	8.56	378
8.7435	846	8.7973	851	8.743	---

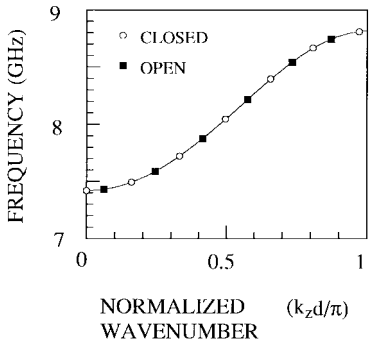

Fig. 2. The resonance frequencies and the corresponding axial wavenumbers for a six-period open periodic cavity (solid rectangles, ■) and a six-period closed periodic cavity (open circles, ○. See also [4]).

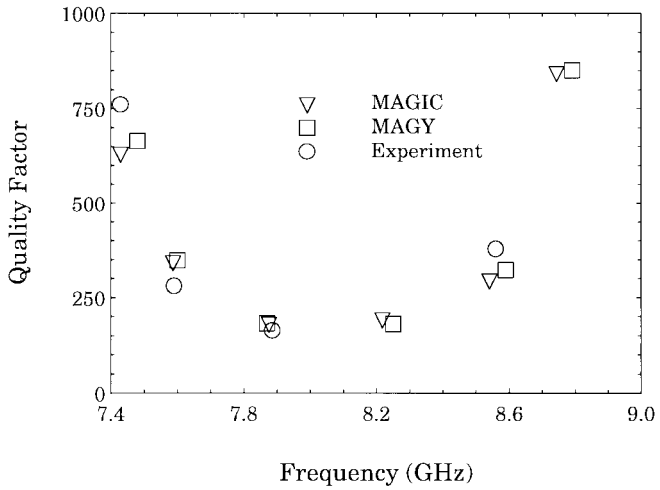

Fig. 3. The measured and calculated quality factors for the six axial modes of the open-periodic cavity. For comparison, the quality factor of the axial modes of a closed periodic cavity are ≈ 2000.

closed cavity, for which the group velocity is zero, are slightly shifted in the open periodic cavity and we obtain a zero-like $(k_z d/\pi = (0+1/2))$ and π-like $(k_z d/\pi = (5+1/2))$ modes with a nonvanishing group velocity. As can be expected, the extraction of energy from the open cavity reduces the value of the quality-factors of the different modes. This is especially noticed for the central $(n = 2, 3, 4)$ modes, while the π-like and zero-like modes maintain a relatively high Q value.

The experimental measurements were compared with numerical simulations. We used the MAGIC code [22] and the newly developed MAGY code [23]. In Fig. 3, we show the quality-factors of the six longitudinal modes as obtained in the experiment and as calculated by MAGY and MAGIC. The values are also listed in Table I. The agreement of the resonance frequencies between the experimental results and the numerical simulations is better than 0.3%. To obtain these values we run MAGY using basis of ten and 20 TM_{0n} modes for the description of the fields. We then extrapolated the computed values of the resonance frequencies for each axial mode using the $1/n_{\mathrm{mod}\,es}$ dependency on the number of modes (see [21] for a detailed discussion of this point). The calculated values for the quality factors agree with the experimental results to better than 10%.

We now proceed to the detailed comparison between the measured and calculated field profile. Using the perturbation technique we measured the frequency shift for each axial mode separately as a function of the axial position of the bead, and computed this shift using MAGY and (4). The results are depicted in Fig. 4(a)–(f) for all six axial modes of the lowest TM_{01} mode of the X-band structure (circles for experimental results and solid line for numerical simulation). The agreement between the measurement and the simulation is excellent, establishing thus the conclusion that this method can be accurately applied for the open-periodic cavity as well. Further, the number of peaks in the frequency shift matches the index of axial mode just like in a closed cavity with reflecting plates at the wide radii. The frequency shift, as given by (4), is a combination of the energy stored in the perturbed electric field and the magnetic field. The frequency shift is always negative, indicating that the contribution of the electric field is dominant over the contribution of the magnetic field [see (4)].

Based on the results of the comparison shown in Fig. 4, we can use the numerical simulations for calculating the electromagnetic field. The current and voltage amplitudes for the dominant TM_{01} mode for the zero-like axial mode are shown in Fig. 5. The envelope of the current amplitude closely resembles the form $\sin[(n+1/2)\pi z/l]$ (l is the length of the line) in order to satisfy the boundary conditions on both ends. This behavior is characteristic of a transmission line with one shorted end and one open end and is the origin of the "half-

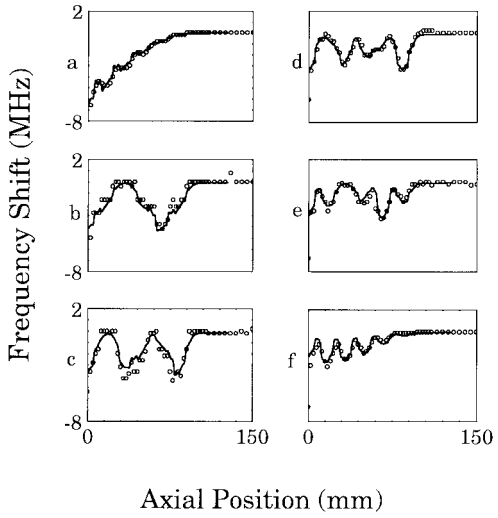

Fig. 4. The frequency shift as a function of axial position for each of the six axial mode of the six-periods open-cavity. (a) $n = 0$, (b) $n = 1$, (c) $n = 2$, (d) $n = 3$, (e) $n = 4$, (f) $n = 5$). Open circles ($\circ$) represent the measured data, while the solid lines (—) are the results of the MAGY calculation.

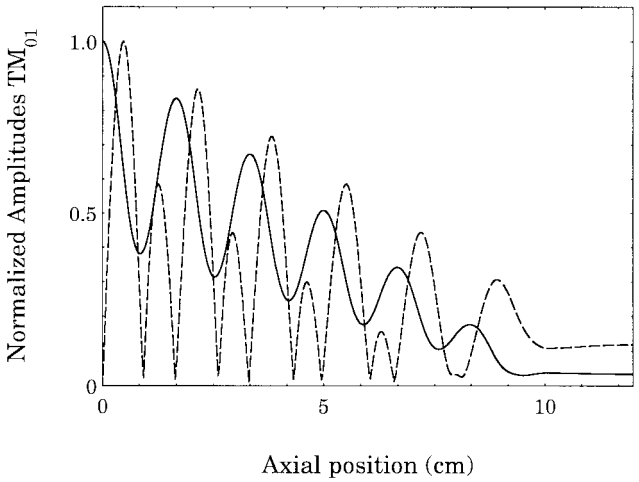

Fig. 5. The current (solid line) and voltage (broken line) amplitudes for the dominant TM_{01} mode for the zero-like axial mode.

integer" spacing between adjacent axial modes in the open periodic cavity.

IV. Wide-Band Matching of a Corrugated Cavity to a Radiating Antenna

Our results for the open periodic cavity clearly show that the coupling to a radiating antenna reduces the value of the quality factor from about $Q \approx 2000$ in the closed cavity [4] to the range of $250 < Q < 800$. Furthermore, Q strongly depends on the operating frequency (alternatively, of the axial mode) within the passband of the slow wave structure.

For high-power microwave generators, like a BWO, there is often a need to simultaneously increase the start oscillation current over very wide frequency band while maintaining an optimal coupling to a radiation extraction antenna. Both goals can be achieved by lowering the quality factors of the cavity over the required bandwidth. In this section we demonstrate that a *short* matching interface between the cavity and the

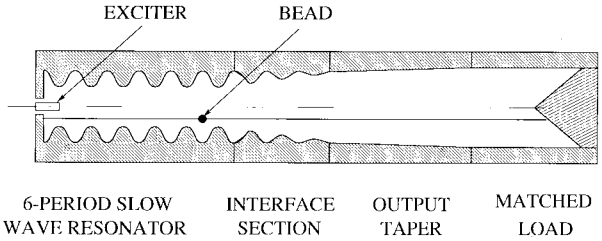

Fig. 6. A schematic diagram of the open periodic cavity with the tapered matching section and the experimental setup used for the frequency and field profile measurements (see text for details).

radiating antenna (load) can substantially reduce the quality factor over most of the useful cavity passband. In the design of the matching section we had two main guidelines.

1) The matching section is kept as short as possible so that the interaction of the waves with an electron beam there will be small. However, there is a tradeoff between this requirement and the need for a gradual transition from the corrugated section to the tapered one, to reduce the electromagnetic reflections.
2) The large radius of the matching section is kept constant and equal to the large radius of the corrugated section (i.e., $R_{\max} = R_0 + h$). Accordingly, both the average radius and corrugation depth must be a function of the axial position.

In view of these guidelines, we chose the length of the matching-section to be three periods of the corrugated cavity, as shown schematically in Fig. 6, and three different types of corrugation-tapering were tested (see Table II).

Three types of measurements were performed for each matching section, using an experimental setup similar to that described in Section II. Hence we obtained the resonance frequencies, the Q values, and the field profile (frequency shift). The resonance curves associated with the three matching-sections are shown in Fig. 7(b)–(d) for the linear, power, and exponential cases, respectively. For comparison we show the resonance curve for the open periodic cavity with no matching section [Fig. 7(a), similar to Fig. 2(a) above]. The effect of the matching-section on the different axial modes is clearly evident. The resonance-width of the central modes is much wider while the frequency is almost unchanged. The zero-like and π-like modes are affected to a lesser degree. While the resonant frequencies are almost identical in all four cases, the Q's are substantially reduced by the matching sections. The quality factor for each axial mode, calculated from the experimental data, is plotted in Fig. 8. The measured quality factors achieved by the linear and exponential tapers are very low, close to the diffraction limit $(Q_{\text{diff}} \approx 60)$ except for the zero-like and π-like modes. This results clearly demonstrate a cavity-load matching over wide-frequency band (7.5–8.6 GHz).

V. Discussion and Summary

The electromagnetic properties of open periodic cavities, which serve as slow-wave resonators for high-power relativistic BWO tubes, have been experimentally and theoretically

TABLE II
THREE TYPES OF MATCHING SECTIONS USED TO REDUCE QUALITY FACTORS OF AN OPEN CORRUGATED CAVITY. HERE $R_{\min}^{(0)}$ IS THE MINIMUM RADIUS OF THE UNIFORM PERIODIC SECTION, $R_{\min}^{(n)}$ IS THE MINIMUM RADIUS OF THE nTH PERIOD OF THE MATCHING SECTION $(n = 1, 2, 3)$, $R_0 = 1.494$ cm, AND $0 \le z \le 3d$

TAPER TYPE	$\frac{R_{\max} - R_{\min}^{(n)}}{R_{\max} - R_{\min}^{(0)}}$	R_{wall}
Linear	1-(2n-1)/6	$R_0 \exp(0.0474z) + h\left(1 - \frac{z}{5.02}\right)\cos\left(2\pi \frac{z}{d}\right)$
Power of 2	$1/2^n$	$\left(R_0 + 0.001327z^5 - 0.02088z^4 + 0.1254z^3 - 0.3574z^2 + 0.51025z\right) + h\exp(-0.6z)\cos\left(2\pi \frac{z}{d}\right)$
Exponential	exp(-n)	$R_0 \exp(0.042z) + h\exp(-0.4022z)\cos\left(2\pi \frac{z}{d}\right)$

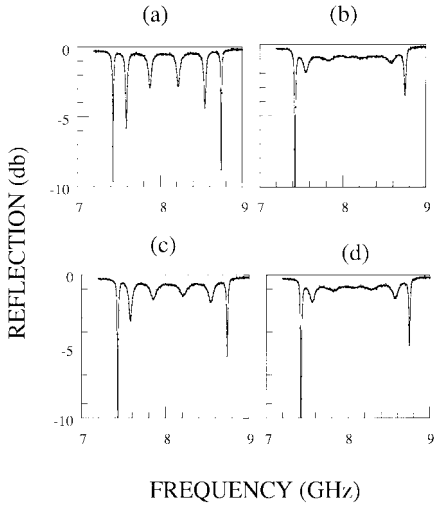

Fig. 7. The measured resonance frequency curve for an periodic cavity with: (a) no matching section; (b) linear matching section; (c) power-of-two matching section; and (d) exponential matching section.

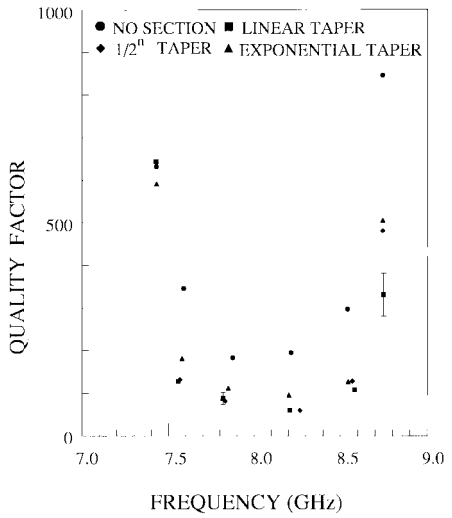

Fig. 8. The measured quality factors for each axial modes for the three different matching sections in an open periodic cavity.

studied, and compared to those of closed cavities. Specifically, the following issues were addressed in a six period $(N = 6)$ open periodic cavity: 1) the number of axial modes associated with the TM_{01} mode; 2) the resonance frequencies; 3) the quality factors; and 4) the field profile associated with each of these modes.

In contrast to closed cavities, where the number of axial modes is equal to $(N + 1)$, an open periodic cavity supports only N axial modes. The spacing of these modes was shown to conform with the "half-integer" spacing, and this was attributed to the different boundary conditions at the open end. It was also shown that the open cavity can not support the exact zero and π modes of the closed cavity, but only zero or π-like modes with a nonvanishing group velocity. This "half-integer" spacing causes a substantial frequency shift for each of the longitudinal modes in an open, as compared to a closed cavity. Furthermore, in open corrugated cavities the quality factors are dominated by radiation extraction through the opening and not by the ohmic wall losses.

The resonance frequencies associated with each of the six axial modes of an open cavity were measured and computed by two different codes, namely MAGIC and MAGY. We found an agreement of better than $\pm 0.3\%$ between the measured resonance frequencies and the values calculated by MAGY and MAGIC codes. Further, the quality factors associated with each of the six axial modes were measured and compared to the numerical simulations with an agreement better than $\pm 10\%$.

As a more detailed study of the field profile of the various axial modes in an open cavity, we used the perturbation technique. It was shown that this method, which is commonly used for closed cavities, can be successfully applied for open cavities. To perturb the cavity, a small aluminum bead was placed at known locations within the structure. The resonance frequency in the open cavity was then recorded as a function of the bead position. The resulting frequency shift (Δf) at a given position corresponds to the local field profile (more specifically the profile of the energy density). Measurements of frequency shift were performed for each of the six axial

modes and found to be in agreement (typically better than 0.01%) with the MAGY calculation. Furthermore, one can find the longitudinal wavenumber associated with each axial mode by counting the number of local maxima in the curve of the frequency shift along the length of the resonator, much in the same way as in a closed cavity.

Finally, we experimentally demonstrated that a significant reduction of the quality factors of the axial modes over a wide range of frequencies, can be obtained by using a matching section. A short tapered periodic interface structure (total length of three periods), for which the tapering were either linear, powers of two, or exponential, was used. The quality factors of the axial modes was drastically reduced down to the diffraction limit. This reduction in Q is expected to substantially increase the starting current (I_{st}) since $I_{st} \propto 1/Q$. This is very beneficial for high-power microwave devices since it allows operation at substantially higher beam (I_b) currents and still satisfying the condition $I_b/I_{st} \approx 23$. It was shown that operating above this critical value leads to a gradual degradation of the spectral purity [27] of the electromagnetic radiation, culminating in the onset of stochastic oscillations. Furthermore, this will allow continuous frequency tunability, by changing the beam voltage without frequency hopping from one axial mode to another. This important feature of the tapered matching section still need to be studied to find the best tapering for a given structure.

In conclusion, this work demonstrates the applicability of combined theoretical and experimental techniques needed for a thorough understanding of the cold-mode structure of an open-periodic cavity. This newly available information is expected to enhance the capability of designing high-power microwave sources.

ACKNOWLEDGMENT

The authors would like to acknowledge the helpful discussion with G. Nusinovich and the help of J. Pyle.

REFERENCES

[1] N. Kovalev, M. I. Petelin, M. D. Reizer, A. V. Smorgonsky, and L. Tsopp, "Generation of powerful electromagnetic radiation pulses by a beam of relativistic electrons," *JEPT Lett.*, vol. 18, pp. 138–140, 1973.
[2] Y. Carmel, J. Ivers, R. E. Kribel, and J. Nation, "Intense, coherent Cerenkov radiation due to the interaction of a relativistic beam with a slow wave structure," *Phys. Rev. Lett.*, vol. 33, p. 21, 1974.
[3] J. A. Swegle, J. W. Poukey, and G. T. Leifeste, "Backward wave oscillators with rippled wall resonators: Analytic theory and numerical simulation," *Phys. Fluids*, vol. 28, pp. 2882–2894, 1985.
[4] C. C. Johnson, *Field and Wave Electromagnetics*. New York: McGraw-Hill, 1965, ch. 7.
[5] W. Main, Y. Carmel, K. Ogura, J. Weaver, G. Nusinovich, S. Kobayshi, J. P. Tate, J. Rodgers, A. Bromborsky, S. Watanabe, M. R. Amin, K. Minami, W. Destler, and V. L. Granatstein, "The electromagnetic properties of open and closed corrugated cavities," *IEEE Trans. Plasma Sci.*, vol. 22, p. 5, 1994.
[6] Y. Carmel, H. Guo, W. R. Lou, D. Abe, V. L. Granatstein, and W. W. Destler, "Novel method for determining the electromagnetic dispersion relation of slow wave structures," *Appl. Phys. Lett.*, vol. 57, pp. 1304–1306, 1990.
[7] B. Levush, T. M. Antonsen, Jr., A. N. Vlasov, G. Nusinovich, S. M. Miller, Y. Carmel, V. L. Granatstein, W. W. Destler, A. Bromborsky, C. Schlesiger, D. Abe, and L. Ludeking "High efficiency relativistic backward wave oscillators: Theory and design," *IEEE Trans. Plasma Sci.*, vol. 24, p. 3, 1996.
[8] B. Levush, T. M. Antonsen Jr., A. Bromborsky, W. Lou, and Y. Carmel, "Theory of relativistic backward wave oscillator with end reflections," *IEEE Trans. Plasma Sci.*, vol. 20, p. 263, 1992.
[9] ———, "Relativistic backward wave oscillators: Theory and experiment," *Phys. Fluids B*, vol. 4, p. 2293, 1992.
[10] S. M. Miller, T. M. Antonsen, Jr., B. Levush, A. Bromborsky, D. K. Abe, and Y. Carmel, "Theory of relativistic backward wave oscillators operating near cutoff," *Phys. Plasmas*, vol. 1, p. 730, 1994.
[11] A. Bromborsky, *SPIE Intense Microwave Part. Beams III*, vol. 1629, p. 182, 1992.
[12] L. D. Moreland, E. Schamilogolu, R. W. Lemke, A. M. Roitman, S. D. Korovin, and V. V. Rostov, "Enhanced frequency agility of high-power relativistic backward wave oscillators," *IEEE Trans. Plasma Sci.*, vol. 24, p. 3, 1996.
[13] J. Butler and C. B. Wharton, "Twin traveling-wave tube amplifiers driven by a relativistic backward wave oscillators," *IEEE Trans. Plasma Sci.*, vol. 24, p. 3, 1996.
[14] A. G. Shkvarunets, S. Kobayashi, Y. Carmel, J. Rodgers, T. M. Antonsen, Jr., and V. L. Granatstein, "Operation of relativistic backward wave oscillator filled with a preionized, high density, radially inhomogenous plasma," this issue, p. 646–652.
[15] A. Shkvarunets, S. Kobayashi, J. Weaver, Y. Carmel, J. Rodgers, T. M. Antonsen, Jr., V. L. Granatstein, W. W. Destler, K. Ogura, and K. Minami, "Plasma influence on the dispersion properties of finite length corrugated cavities," *Phys. Rev. E*, vol. 53, p. 2045, 1996.
[16] D. M. Goebel, J. M. Butler, R. W. Schumacher, J. Santoru, and R. L. Eisenhart, "High-power microwave source based on an unmagnetized backward wave oscillator," *IEEE Trans. Plasma Sci.*, vol. 22, 1994.
[17] L. Shenggang, J. K. La, S. Liqun, Y. Yang, and Z. Dajun, "Theory of wave propagation along corrugated waveguide filled with plasmas immersed in an axial magnetic field," *IEEE Trans. Plasma Sci.*, vol. 24, 1996.
[18] L. A. Mitin, V. I. Perevodchikov, M. A. Zavyalov, V. N. Tskai, and A. L. Shapiro, "High-power wide-band beam-plasma amplifiers and generators," *Plasma Phys. Rep.*, vol. 20, p. 662, 1994.
[19] L. C. Maier and J. C. Slater, "Field strength measurements in resonant cavities," *J. Appl. Phys.*, vol. 23, pp. 68–77, 1952.
[20] O. P. Gahdhi, *Microwave Engineering and Applications*. Oxford, U.K.: Pergamon, 1984.
[21] W. R. Smythe, *Static and Dynamic Electricity*, 3rd ed. NY: McGraw-Hill, 1967, pp. 535–536.
[22] MAGIC, developed by Mission Research Corp., Newington, VA, B. Goplen *et al.*
[23] M. Botton, T. M. Antonsen, Jr., B. Levush, and A. Vlasov, "MAGY: A quasithree dimensional time dependent code for simulation of electron beam systems," *IEEE Trans. Plasma Sci.*, vol. 26, 1998.
[24] D. K. King, *Measurement at Centimeter Wavelength*. New York: Van Nostrand, 1952, pp. 128–141.
[25] L. Malter and G. A. Brewer, *J. Appl. Phys.*, vol. 20, p. 10, 1949.
[26] L. A. Weinstein, *Open Resonators and Open Waveguides*. Boulder, CO: Golem, 1969, ch. 5.
[27] Y. Carmel, W. R. Lou, J. Rodgers, H. Guo, W. W. Destler, V. L. Granatstein, B. Levush, T. Antosnen, Jr., and A. Bromborsky, "From linearity toward chaos: Basic studies of relativistic backward-wave oscillators," *Phys. Rev. lett.*, vol. 69, p. 11, 1992.

Satoru Kobayashi, photograph and biography not available at the time of publication.

M. Botton, photograph and biography not available at time of publication.

Yuval Carmel (S'66–M'69–SM'90), for a biography, see this issue, p. 604.

Thomas M. Antonsen, Jr., (M'87), for a biography, see this issue, p. 425.

John Rodgers, for a biography, see this issue, p. 460.

Anatoly G. Shkvarunets, for a biography, see this issue, p. 627.

Alexander N. Vlasov (M'95), for a photograph and biography, see this issue, p. 614.

L. Duan, photograph and biography not available at the time of publication.

Victor L. Granatstein (S'59–M'64–SM'86–F'92), for photograph and biography, see this issue, p. 459.